 https://doi.org/10.3311/PPee.23416

Periodica Polytechnica Electrical Engineering and Computer Science, 68(3), pp. 232–239, 2024

Voltage Error Estimation-Based Fault Diagnosis Method for Three- phase PWM-inverter in Grid-connected Photovoltaic Power System Without any Over-rating

Atallah Ouai[1*], Lakhdar Mokrani[1], Mohamed Machmoum[2], Azeddine Houari[2]

[1] LACoSERE Laboratory, Department of Electrical Engineering, Faculty of Technology, University Amar Telidji of Laghouat, P. O. B. 37, Ghardaia Street, 03000 Laghouat, Algeria
[2] IREENA Laboratory, University of Nantes, 37 Boulevard de l'Université, P. O. B. 406, 44602 Saint-Nazaire, Nantes, France
[*] Corresponding author, e-mail: a.ouai@lagh-univ.dz

Received: 11 September 2023, Accepted: 03 February 2024, Published online: 09 May 2024

Abstract

Inverter is an essential component of a grid connected PV system. In fact, an open-switch fault in this power converter could result an important system malfunction and consequently leads to system disconnection. In this context, this paper focuses on the fault-tolerant control of PWM-inverter with redundancy leg for grid-connected PV system. In addition, a fast method of fault detection and compensation is used to maintain the continuous operation of the converter when there is a half-leg open-circuit fault (IGBT+ anti-parallel diode) on one of PWM-inverter legs. Therefore, it can detect this type of fault and compensate it in less than 50 µs by using a time criterion instead of voltage criterion. Also, the fuzzy logic technique is employed to control the active and reactive power injected into the network without exceeding the whole system power capacity limits. Note that, in this study, the active and reactive power references of the chosen operating point (the reactive-to-active power ratio: $tg\varphi = Q/P = 0.19$) are based on experimental tests. Simulation results show the feasibility and the effectiveness of the proposed fault diagnosis method in terms of fault detection and service continuity in presence of a half-leg open-circuit fault in PWM-inverter without any over-rating of the PV system components or instability.

Keywords

photovoltaic generator, inverter half-leg open-circuit fault, fault detection, whole system power capacity limits, active power control, reactive power control, without over-rating

1 Introduction

Over the past decade, and in order to reduce the pollution problem, a lot of effort has been focused on the development of environmentally friendly sources of energies such as wind and solar [1]. Elsewhere, the most of solar photovoltaic energy technologies are used in grid connected power generation system. However, in grid-connected PV systems, the photovoltaic energy conversion is mainly based on numbers of power electronics converters which are considered as the most vulnerable parts in a photovoltaic system and the failure of these converters has very serious consequences on the overall system operation [2]. In fact, a sudden failure in one of the power switches decreases system performances and leads to disconnecting the system. Moreover, if the fault is not quickly detected and compensated, its effect can lead to hard failure of the system [3]. Hence, a tolerant control strategy is extremely important to realize the high reliability requirement of the equipment, ensure continuity of service, and achieve a faster corrective maintenance. According to statistics, the majority of failures are related to faults in electrolytic capacitors and power switches [4]. Many works have discussed the fault tolerant control schemes in power electronic converters for PV systems. A fault diagnosis in the power conversion stage (classical DC-DC boost converter + voltage-source full-bridge inverter) of a grid-connected PV system has been studied in [5]. The proposed fault diagnosis approach is based on the frequency spectrum of the signals in order to achieve faster preventive maintenances. In [6], a redundancy based three-level boost DC converter having fault tolerant capacity is presented. The onverter developed in this work has three states which are described as normal state, faulty state and rebuilt state.

Cite this article as: Ouai, A., Mokrani, L., Machmoum, M., Houari, A. "Voltage Error Estimation-Based Fault Diagnosis Method for Three- phase PWM-inverter in Grid-connected Photovoltaic Power System Without any Over-rating", Periodica Polytechnica Electrical Engineering and Computer Science, 68(3), pp. 232–239, 2024. https://doi.org/10.3311/PPee.23416

In [7], the authors suggested a fault detection diagnosis for the T-type three level inverter that is based on the mass center of the voltage pattern. In reference [8], a new fault detection method is proposed to provide an open-switch fault-tolerant control for both of boost converter and grid-side converter (GSC) in a grid-connected photovoltaic. In this work, the mean value of the error voltages is used as fault indicator for the GSC, while, for the boost converter the inductor current form is used as fault indicator. Also, the author of [9] discussed the open-switch fault case and current sensor fault case in the interleaved flyback converters of a micro-inverter system. Moreover, a solution for modelling and controlling the operation of DC/DC converters, both in normal and in fault regime, is proposed in [10]. The proposed converter model is based on ARX structure with variable coefficients. However, in order to generate the appropriate model coefficients for variable duty cycle, a feedforward neural network is used in this structure. In [11], the authors suggested a new procedure for detecting the faults which occur in the inverter and LCL filter operation for photovoltaic panels application. In this contribution, the load parameters are estimated in real time using a fast estimation method. More recently, in [12], an overview of the research work done in fault tolerant power electronics circuits in photovoltaic applications has been presented. Finally, in [13], a new fault-tolerant control strategy is exposed in a photovoltaic system based on a non-isolated DC-DC converter. The principle of the proposed fault detection method is based on sampling the voltage across the inductor at a much higher frequency than the switching frequency.

Besides, this work aims to study the fault tolerant control of a three-phase PWM-inverter dedicated to pilot grid-connected PV system. The fault tolerant topology DC-AC converter is applied by adding one redundant leg and associated with fast method of fault detection and compensation to maintain the service continuity, when a half-leg open-circuit fault occurs on the level of one of its legs. The suggested method minimizes the delay time between the fault occurrence and its compensation. Simulation results show the effects of half-leg open-circuit fault on the studied PV system response and demonstrate the possibility to compensate it in less than 50 µs by using a time criterion instead of voltage criterion and therefore with such a fault tolerant topology, the PV system can stay safely connected to the network under fault conditions.

The rest of the paper is organized as follows. Section 2 gives a description of the studied grid connected PV system. A modeling of a PCS and a proposed fault tolerant detection method are detailed in Section 3.

Simulation results are presented and discussed in Section 4. Section 5 is devoted to conclusion.

2 System description

Fig. 1 [14] represents the configuration of HMSS (Hokuto Mega-Solar System) grid connected. From this structure, our study is focused on the 400 kW Power Conditioning System (PCS) of the 2nd stage, which is consisted of a 400 kW inverter and two 200 kW choppers as shown in Fig. 2 [15]. The technical specifications of the PCS are listed in Table 1 [15–17].

3 Modeling and control of 400 kW PCS

In this work, the issues which need to be addressed by the 400 kW Large Scale (LS)-PCS control are:

- Capture of maximum energy from the solar (MPPT);
- Inject the active and reactive power into the grid;

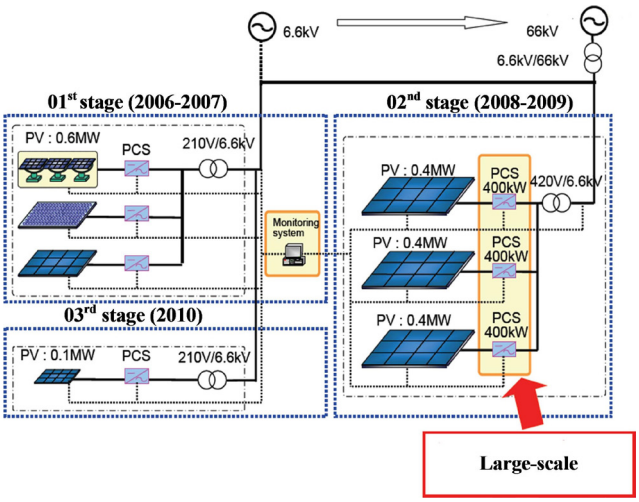

Fig. 1 Structure of HMSS connected to the grid [14]

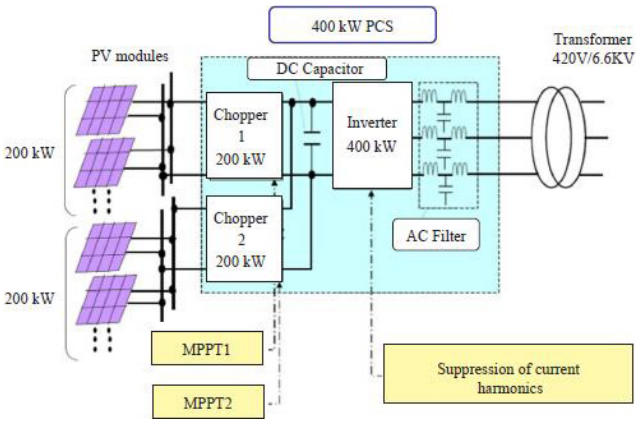

Fig. 2 PCS configuration [15]

Table 1 Specification of PCS [15]

Capacity	420 kVA / 400 kW
AC voltage	420 V ± 10%
DC voltage	600 V
Input DC voltage	230–600 V
Switching frequency	4 kHz
Conversion efficiency	> 95%
Control functions	MPPT by choppers Suppression of low-order harmonics

- Ensure the service continuity in presence of PWM-inverter half-leg open-circuit fault without exceeding the whole system power capacity. The control scheme of the LS-PCS grid-connected is depicted in Fig. 3. To operate the LS-PCS in the MPPT mode in order to capture the maximum power from the solar, the DC-DC boost converter has been controlled using a pilot cell technique proposed in [17]. Moreover, to ensure an active and reactive power control, two fuzzy logic controllers (FLC1 and FLC2) are used (see Fig. 4).

The instantaneous active and reactive power delivered to the grid can be written as follows [18]:

$$\begin{cases} P = \frac{3}{2}\left(v_d i_d + v_q i_q\right) \\ Q = \frac{3}{2}\left(v_q i_d - v_d i_q\right) \end{cases}. \quad (1)$$

So, to control the active power P by tuning the FLC1, the reference current (i_{dref}) is derived from the active power error e_P and its variation Δe_P which are defined as [19, 20]:

$$e_p = P_{ref} - P, \quad (2)$$

$$\Delta e_p = \left(1 - z^{-1}\right) e_p. \quad (3)$$

Also, the control of the reactive power Q to follow a desired value (Q_{ref}) is achieved by tuning FLC2 on the reference current (i_{qref}) as shown in Fig. 3. Hence, the reactive power error e_Q and its variation Δe_Q are given by:

$$e_Q = Q_{ref} - Q, \quad (4)$$

$$\Delta e_Q = \left(1 - z^{-1}\right) e_Q. \quad (5)$$

Thus, the discrete form of the outputs of the two fuzzy controllers is given as follows in the dq frame:

$$i_{dref}\left(k+1\right) = i_{dref}\left(k\right) + k_{d\Delta i}\Delta i_{drefn}\left(k+1\right), \quad (6)$$

$$i_{qref}\left(k+1\right) = i_{qref}\left(k\right) + k_{q\Delta i}\Delta i_{qrefn}\left(k+1\right). \quad (7)$$

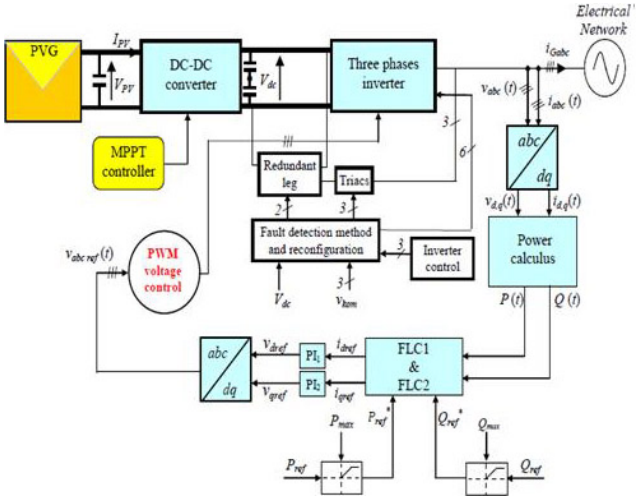

Fig. 3 Control scheme of the LS-PCS for power generation and fault tolerant control

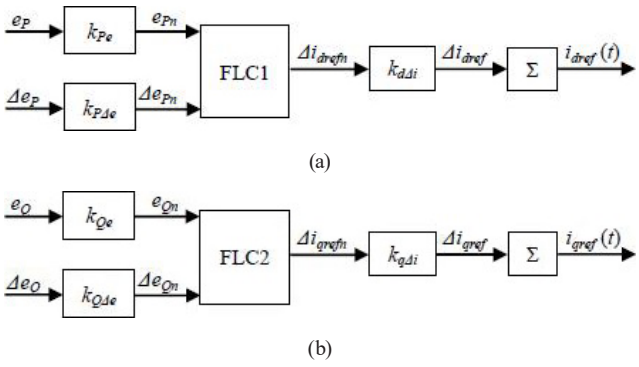

Fig. 4 Active and reactive powers fuzzy logic controllers; (a) Fuzzy logic controller of active power; (b) Fuzzy logic controller of reactive power

3.1 PV system power capability

The capacity of the PV system is delimited in the plan (PQ) to avoid overloading of the constituent elements throughout the solar conversion chain. The hatched area (green trapeze in Fig. 5) represents the limits of the whole PV system capacity (T = 25 °C and G = 1000 W/m^2) in terms of active and reactive powers injected into the grid.

3.2 Fault-tolerant PWM-inverter topology

Several topologies of DC-AC converters are used in power electronic applications. Fig. 6 shows the studied fault-tolerant topology. It is based on a redundant leg composed of the switches T_7 and T_8. This leg will replace the faulty one of the other legs under any power switch failure in the PWM-inverter. When a fault occurs in one of the power switches ($T_1 - T_6$), the fault detection scheme detects the fault occurrence and isolates the faulty leg [21]. If this fault is an open circuit, the isolation is implemented by removing the gate signal from the switches of the faulty leg. In the case of short circuit, the faulty leg is isolated by fast acting fuses and consequently, the short-circuit fault becomes

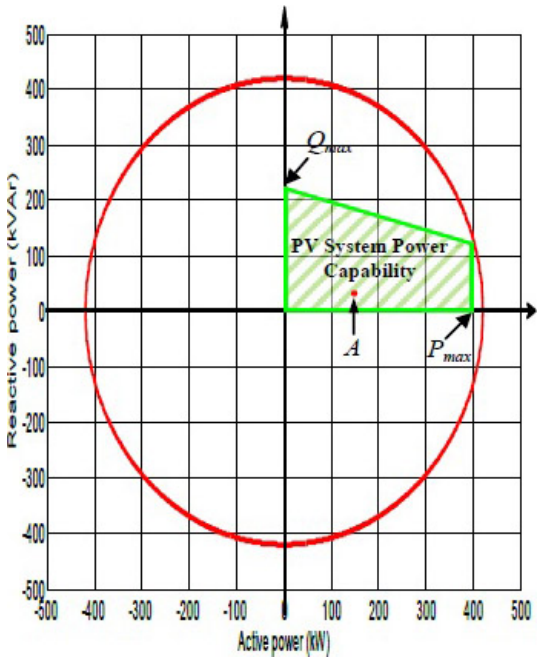

Fig. 5 Active and reactive powers limits of the studied PV system

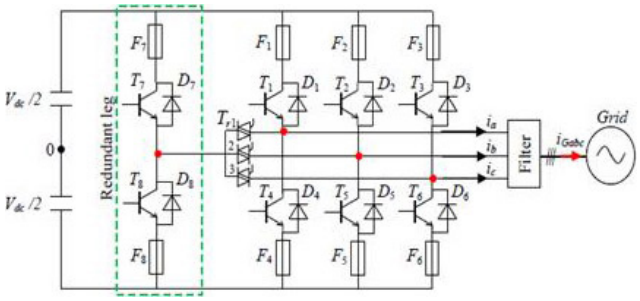

Fig. 6 Fault tolerant topology of PWM-inverter with redundancy leg

an open-circuit fault after isolation of the faulty leg by the two fuses. In both cases, the reconfiguration scheme triggers the suited bidirectional switch (*TRIAC*) to connect the faulty phase to the midpoint of the redundant leg.

In brief, in a fault case on the leg number k (k = 1, 2, 3), the compensation is achieved by the following steps [22]:

1. Detection of the fault and therefore the faulty leg (detailed in next paragraph);
2. Removing the switching orders of the two switching drivers of the faulty leg;
3. Close the suited bidirectional switch by activating its command;
4. Using the switching orders of the faulty leg for the redundant one;
5. Stopping the fault detection scheme.

3.3 Fault detection scheme

In this study, the fault detection method is based on the comparison between measured and estimated pole voltages of converter, v_{k0m} and v_{k0es} (k = 1, 2, 3), respectively [22, 23]. The estimated voltages v_{k0es} can be expressed by the following equation:

$$v_{k0es} = (2\delta_k - 1)\frac{V_{DC}}{2}, \tag{8}$$

where $\delta_k \in \{0, 1\}$ is the switching pattern of the top semi-conductor switches of the leg number k and V_{DC} is the DC-bus voltage.

An open-switch fault can be detected by analyzing the difference between the measured and estimated voltages. A voltage error, denoted ε_{k0} is therefore defined by:

$$\varepsilon_{k0} = (v_{k0m} - v_{k0es}). \tag{9}$$

In the healthy condition, the pole voltages are equal and thus, their difference is zero. We suppose that the switches are ideal. With this supposition, in normal operation, the measured and estimated pole voltages are equal and thus their difference is zero.

Let us consider that an open-circuit fault occurs in the switch T_k (k = 1, 2, 3) of the leg k.

The equivalent circuit of this faulty leg is illustrated by Fig. 7. In this circuit, the measured pole voltage v_{k0m} and the voltage error ε_{k0} for the phase k depend on the phase current ($i_{Ga,\,b\,or\,c}$ positive or negative) and the switching pattern δ_k, indeed:

- if $i_{Ga,\,b\,or\,c} > 0 \Rightarrow v_{k0m} = -V_{DC}/2$,
- if $i_{Ga,\,b\,or\,c} < 0$ and $\delta_k = 0 \Rightarrow v_{k0m} = -V_{DC}/2$,
- if $i_{Ga,\,b\,or\,c} < 0$ and $\delta_k = 1 \Rightarrow v_{k0m} = V_{DC}/2$.

In addition, Table 2 gathers the analytical expressions of the voltage after the fault occurrence, according to the switching pattern δ_k, when the current $i_{Ga,\,b\,or\,c}$ is different from zero.

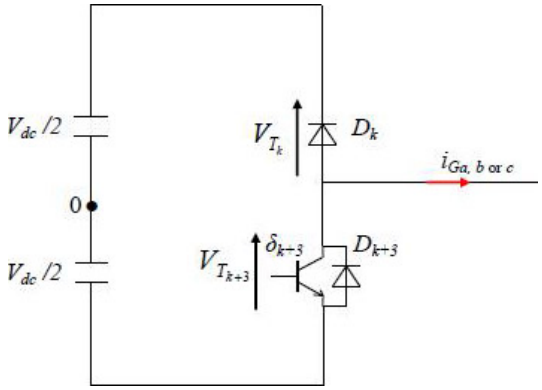

Fig. 7 Equivalent circuit of the leg k in the case of an open-circuit fault in the switch T_k (k =1, 2, 3)

Table 2 Voltage error during an open-circuit fault of the switch T_k

$i_{Ga,\ b\ or\ c}$	δ_k	D_k	D_{k+3}	v_{k0m}	v_{k0es}	ε_{k0}
> 0	1	off	on	$-V_{DC}/2$	$+V_{DC}/2$	$-V_{DC}$
> 0	0	off	on	$-V_{DC}/2$	$-V_{DC}/2$	0
< 0	1	on	off	$+V_{DC}/2$	$+V_{DC}/2$	0
< 0	0	off	off	$-V_{DC}/2$	$-V_{DC}/2$	0

Up to now, we supposed that the switches are ideal. In this hypothesis, the previous analytical study demonstrated that the possible fault of a switch can be detected by a simple comparison between the measured voltage vk0m and the estimated voltage v_{k0es}. However, in real case, because of turn-off and turn-on propagation time and interlock dead time generated by the switches drivers, the voltage error ε_{k0} is not null and constituted of peaks during switching time [22, 23]. In fact, to avoid the detections errors due to semiconductor switching, the absolute value of the voltage error $|\varepsilon_{k0}|$ is firstly compared with the threshold value '*h*', to determine if the difference between the measured and estimated voltages is large enough to be considered a fault as shown in Fig. 8.

The output of the first comparator, noted C_k is equal to 0 if $|\varepsilon_{k0}| < h$ and equal to 1 if $|\varepsilon_{k0}(t)| \geq h$. Thus, the signal at the output of this comparator has a square waveform with a low duty cycle and a frequency equal to twice the switching frequency of the switches. If, we inject this output into an integrator, we obtain the time during which v_{k0m} and v_{k0es} are different if the integration is initialized to zero after each square waveform. This is done using a counter which receives the signal C_k and delivers an image of the time nk. To detect the fault, the integrated resulting signal is applied to a second comparator having a threshold value N_t several times larger than the switching time T_s. In this way, false fault alerts due to semiconductor switching are avoided and the fault can be detected in less than 30 µs (this time includes delays due to acquisition and switching time) [24].

The resulting signal (noted by OCF_T_k: Open-Circuit Fault in the switch T_k) of the open-circuit fault detection scheme is used to isolate the faulty leg, trigger the suited switch T_{rk} (k = {1, 2, 3}) and stop the fault detection.

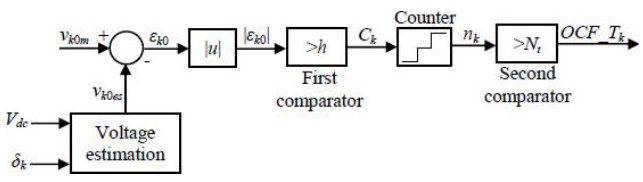

Fig. 8 Block diagram of the fault detection method

4 Simulation results

Results of simulation study allowed us to understand the dynamic of the proposed PV system connected to power network which is assumed as stable and balanced.

Firstly, the consequences caused by the occurrence of an open-switch fault in one of PWM-inverter legs are discussed for an operating point (P_{ref}, Q_{ref}), which are based on experimental tests: $tg\varphi = Q/P = 0.19$, see Fig. 7 [17]. Then, the performance of PV system by integrating fault tolerant topology with a redundant leg and a fault detection and compensation procedure is presented to guarantee the service continuity without any over-rating of the PV system power capability.

4.1 Functioning in inverter failure mode

In the following, we will discuss the effects and consequences of a half-leg open-circuit failure on one of PWM-inverter legs without applying the fault-tolerant control strategy (i.e., without fault detection or compensation). Then, we will show the importance and the contribution of the detection techniques and compensation of this type of faults presented previously.

4.1.1 Case of open half-leg without detection and compensation

In this case, an open-circuit fault is considered in the upper half-leg (IGBT (T_1) with the anti-parallel diode (D_1)) of the first leg of the inverter at t = 0.5 s. Fig. 9 shows the simulation results obtained before and after the appearance of this fault at time t = 0.5 sec without introducing fault detection and compensation procedure.

The objective of this simulation test is to show the importance and justify the use of a fault-tolerant control of the PV system connected with the network. Before the fault occurrence (t < 0.5 s), the PV system works correctly. Indeed, the active and reactive powers properly follow their references and the DC bus voltage is stable. On the other hand, as soon as the fault appears, these same powers are no longer correctly controlled and significant oscillations can be noted (see Fig. 9 (a)). Likewise, the DC bus voltage shows unacceptable oscillations and completely collapses as illustrated in Fig. 9 (d).

It is also seen that this fault leads to the total loss of control of the phase current of the faulty leg as shown in Fig. 9 (b). This has repercussions on the other currents which manifest distortions and excessive increases (see Fig. 9 (b) and (c)).

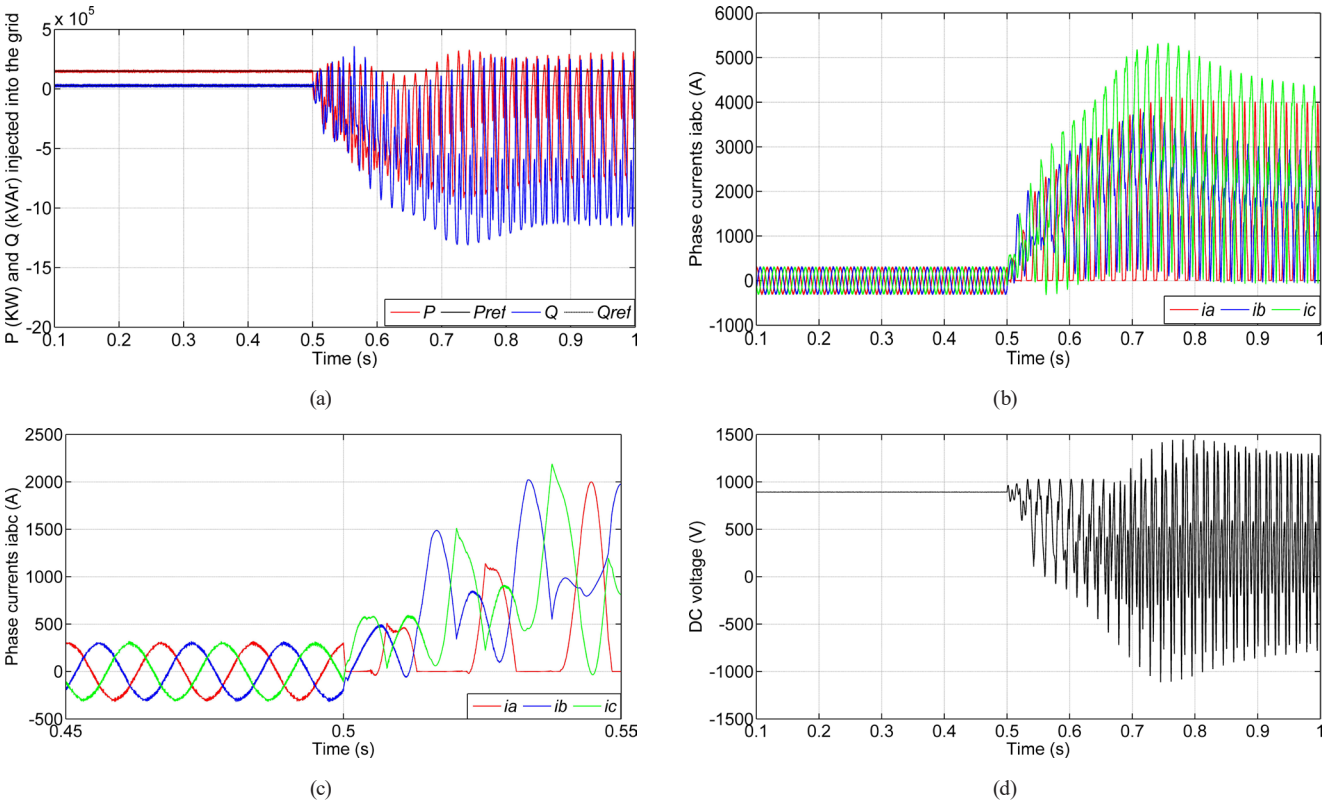

Fig. 9 Simulation results of the studied PV system, case of an open half-leg at $t = 0.5$ s without fault detection or compensation; (a) Active power (kW) and reactive power (kVAr); (b) Phase currents i_{abc} (A); (c) Zoom of iabc (A); (d) V_{DC} bus voltage (V)

Thus, if the fault is not quickly detected and effectively compensated, these effects on the PV system will be destructive and destabilizing and the protection systems (circuit breakers, fuses, etc.) will undoubtedly intervene to disconnect the system and anticipate these undesirable effects.

Under these conditions, the service continuity is not ensured.

4.1.2 Detection and compensation of half-leg open-circuit fault

Let us now present the performance of the fault tolerant topology of PWM-inverter based on redundancy leg, with a very fast method of fault detection and reconfiguration as shown schematically in Fig. 8. It can detect the fault and compensate it in less than 50 µs. Simulation results are carried out in the same conditions of failure of a power converter as previously discussed. In this case, the active power injected into the network is slightly influenced by this open-circuit fault in the upper switch. It decreases from 150 kW to approximately 123 kW, then regains its reference in approximately 250 µs, which is the time required to detect and compensate this fault (see Fig. 10 (a)). However, the reactive power injected into the network is not at all influenced by this fault. The same is true for the phase currents (in particular that of phase (a) which marks a deviation of 36 A at the first instants of the fault) as shown in the Fig. 10 (b) and (c). In addition, there is a non-significant peak in the DC bus voltage (about 5 V), see Fig. 10 (d). Thus, the active and reactive powers injected into the network are properly controlled; the phase currents remain practically and the DC bus voltage is well stabilized. In this case, the PV system can tolerate this kind of failure without worries and continue to operate normally.

5 Conclusion

In this paper, an inverter half-leg open-circuit fault-tolerant control in a grid-connected solar PV system has been applied. This control is based on a redundant leg and associated with an affective and fast method of fault detection and reconfiguration. To avoid the over-rating of the studied PV system components during its control for power generation and guarantee the service continuity, its power capacity has been delimited in the (PQ) power plane. In addition, fuzzy logic approach has been used to control the active and reactive power injected into the network.

Simulation results show the effectiveness and rapidity of the proposed method in terms of fault detection and

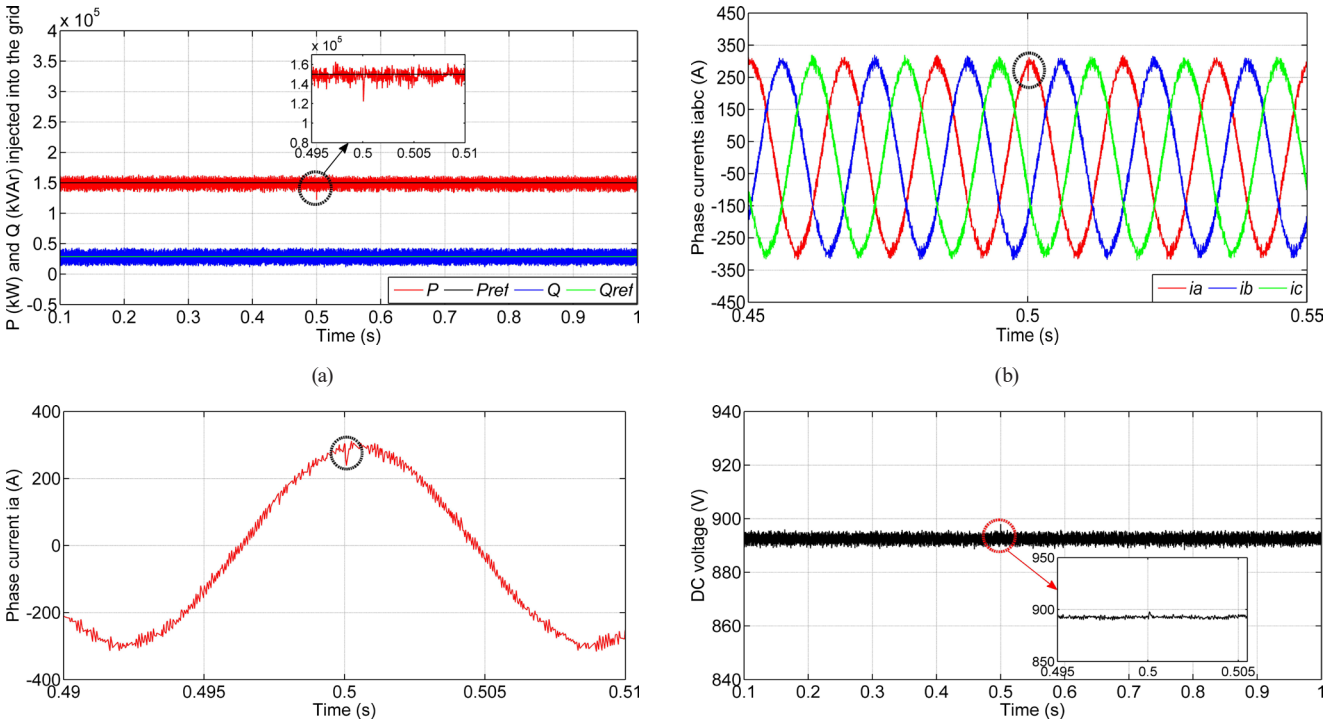

Fig. 10 Simulation results of the studied PV system, case of an open half-leg with fault detection or compensation in 50 µs; (a) Active power (kW) and reactive power (kVAr); (b) Phase currents i_{abc} (A); (c) Zoom of i_a (A); (d) V_{DC} bus voltage (V)

diagnosis. It can detect this type of fault and compensate it in less than 50 µs by using a time criterion instead of voltage criterion. Therefore, the PV system can stay safely connected to the network under fault conditions without over-rating the whole system component or instability.

References

[1] Kumar, M. "Social, Economic, and Environmental Impacts of Renewable Energy Resources", In: Okedu, K. E., Tahour, A., Aissaou, A. G. (eds.) Wind Solar Hybrid Renewable Energy System, 2020, pp. 227–252. ISBN 978-1789845907 https://doi.org/10.5772/intechopen.89494

[2] Kulkarni, N. G., Virulkar, V. B. "Power Electronics and Its Application to Solar Photovoltaic Systems in India", Energy and Power Engineering, 8(2), pp. 76–91, 2016. https://doi.org/10.4236/epe.2016.82007

[3] Shahbazi, M., Poure, P., Saadate, S., Zolghadri, M. R. "FPGA-based Fast Detection with Reduced Sensor Count for a Fault-Tolerant Three-Phase Converter", IEEE Transactions on Industrial Informatics, 9(3), pp. 1343–1350, 2013. https://doi.org/10.1109/TII.2012.2209665

[4] Dhople, S. V., Davoudi, A., Domínguez-Garcia, A. D., Chapman, P. L. "A Unified Approach to Reliability Assessment of Multiphase DC–DC Converters in Photovoltaic Energy Conversion Systems", IEEE Transactions on Power Electronics, 27(2), pp. 739–751, 2012. https://doi.org/10.1109/TPEL.2010.2103329

[5] González, M., Raison, B., Bacha, S., Bun, L. "Fault Diagnosis in a Grid-Connected Photovoltaic System by Applying a Signal Approach", In: IECON 2011 - 37th Annual Conference of the IEEE Industrial Electronics Society, Melbourne, Victoria, Australia, 2011, pp. 1354–1359. ISBN 9781612849690 https://doi.org/10.1109/IECON.2011.6119505

[6] Ribeiro, E., Cardoso A., Boccaletti, C. "Fault-Tolerant Strategy for a Photovoltaic DC–DC Converter", IEEE Transactions on Power Electronics, 28(6), pp. 3008–3018, 2013. https://doi.org/10.1109/TPEL.2012.2226059

[7] Pires, V. F., Foito, D., Amaral, T. G. "Fault Detection and Diagnosis in a PV Grid-Connected T-Type Three Level Inverter", In: 2015 4th International Conference on Renewable Energy Research and Applications (ICRERA 2015), Palermo, Italy, 2015, pp. 933–937. ISBN 9781479999835 https://doi.org/10.1109/ICRERA.2015.7418547

[8] Boudjellal, B., Benslimane, T. "Open-switch Fault-tolerant Control of Power Converters in a Grid-connected Photovoltaic System", International Journal of Power Electronics and Drive System (IJPEDS), 7(4), pp. 1294–1308, 2016. http://doi.org/10.11591/ijpeds.v7.i4.pp1294-1308

[9] Li, Z., Peng, T., Zhang, P., Han, H., Yang, J. "Fault Diagnosis and Fault-Tolerant Control of Photovoltaic Micro-Inverter", Journal of Central South University, 23(9), pp. 2284–2295, 2016. https://doi.org/10.1007/s11771-016-3286-7

[10] Muresan, V., Moga, D., Petreus, D., Abrudean, M., Stroia, N., Moga, R. "Fault Detection and Fault Tolerance Mechanism for DC/DC Converters in Microgrids", IFAC-PapersOnLine, 51(28), pp. 666–671, 2018. https://doi.org/10.1016/j.ifacol.2018.11.781

[11] Muresan, V., Moga, D., Petreus, D., Abrudean, M., Stroia, N., Moga, R. "Fault Tolerant Control System for Photovoltaic Panels Application", IFAC-PapersOnLine, 52(4), pp. 354–359, 2019. https://doi.org/10.1016/j.ifacol.2019.08.235

[12] Chavan, S. B., Bhad, S. A. "An Overview of Fault Tolerant Methods in Power Circuits of Photovoltaic Applications", International Research Journal of Engineering and Technology, 7(6), pp. 4955–4959, 2020. [online] Available at: https://www.irjet.net/archives/V7/i6/IRJET-V7I6931.pdf [Accessed: 11 August 2023]

[13] Abouobaida, H., Abouelmahjoub, Y. "New Diagnosis and Fault-Tolerant Control Strategy for Photovoltaic System", International Journal of Photoenergy, 2021, 8075165, 2021. https://doi.org/10.1155/2021/8075165

[14] Ouai, A., Mokrani, L., Machmoum, M., Houari, A. "Power Quality Improvement of a Solar Energy Conversion System by a Coordinated Active and LCL Filtering", Periodica Polytechnica Electrical Engineering and Computer Science, 65(4), pp. 373–381, 2021. https://doi.org/10.3311/PPee.17215

[15] Ouai, A., Mokrani, L., Machmoum, M., Houari, A. "Control and energy management of a large scale grid-connected PV system for power quality improvement", Solar Energy, 171, pp. 893–906, 2018. https://doi.org/10.1016/j.solener.2018.06.106

[16] Konishi, H. "Study of MPPT Control Method for Large-scale Power Conditioning System in Hokuto Mega-solar System", Journal of International Council on Electrical Engineering, 4(2), pp. 173–178, 2014. https://doi.org/10.5370/JICEE.2014.4.2.173

[17] Konishi, H., Iwato, T., Kudou, M. "Verification test results of 2nd stage in Hokuto mega-solar system", In: 2011 37th IEEE Photovoltaic Specialists Conference, Washington, USA, 2011, pp. 2375–2379. ISBN 9781424499663 https://doi.org/10.1109/PVSC.2011.6186428

[18] Sezen, S., Aktas, A., Uçar, M., Ozdemir, E. "A three-phase three-level NPC inverter based grid-connected photovoltaic system with active power filtering", In: 2014 16th International Power Electronics and Motion Control Conference and Exposition, Antalya, Turkey, 2014, pp. 1572–1576. ISBN 978-1-4799-2061-7 https://doi.org/10.1109/EPEPEMC.2014.6980697

[19] Boutoubat, M., Marmouh, S., Hadjaissa, A. "Grid connected WECS control for power production and power factor correction", In: 2020 1st International Conference on Communications, Control Systems and Signal Processing (CCSSP 2020), El Oued, Algeria. 2020, pp. 406–410. ISBN 9781728158365 https://doi.org/10.1109/CCSSP49278.2020.9151743

[20] Benlarbi, K., Mokrani, L., Nait-Said, M. S. "A fuzzy global efficiency optimization of a photovoltaic water pumping system", Solar Energy, 77(2), pp. 203–216, 2004. https://doi.org/10.1016/j.solener.2004.03.025

[21] Sahraoui, K., Gaoui, B. "Reconfigurable Control of PWM AC-DC-DC Converter without Redundancy Leg Supplying an AC Motor Drive", Periodica Polytechnica Electrical Engineering and Computer Science, 65(1), pp. 74–81, 2021. https://doi.org/10.3311/PPee.15028

[22] Shahbazi, M., Zolghadri, M. R, Poure, P., Saadate, S. "Wind energy conversion system based on DFIG with open switch fault tolerant six-legs AC-DC-AC converter", In: 2013 IEEE International Conference on Industrial Technology, Cape Town, South Africa, 2013, pp. 1656–1661. ISBN 9781467345675 https://doi.org/10.1109/ICIT.2013.6505922

[23] Sahraoui, K., Gaoui, B., Mokrani, L., Belarbi, K. "Fast detection control for fault-tolerant converter back-to-back with redundancy leg supplying an induction motor drives", Journal of Digital Signals and Smart Systems, 2(1), pp. 15–35, 2018. https://doi.org/10.1504/IJDSSS.2018.090869

[24] Karimi, S., Gaillard, A., Poure, P., Saadate, S. "FPGA Based Real-time Power Converter Failure Diagnosis for Wind Energy Conversion Systems", IEEE Transactions on Industrial Electronics, 55(12), pp. 4299–4308, 2008. https://doi.org/10.1109/TIE.2008.2005244